Statistical and Molecular Dynamics Studies of Buried Waters in Globular Proteins

Sheldon Park and Jeffery G. Saven*
Makineni Theoretical Laboratories, Department of Chemistry, University of Pennsylvania, Philadelphia, Pennsylvania

ABSTRACT **Buried solvent molecules are common in the core of globular proteins and contribute to structural stability. Folding necessitates the burial of polar backbone atoms in the protein core, whose hydrogen-bonding capacities should be satisfied on average. Whereas the residues in α-helices and β-sheets form systematic main-chain hydrogen bonds, the residues in turns, coils and loops often contain polar atoms that fail to form intramolecular hydrogen bonds. The statistical analysis of 842 high resolution protein structures shows that well-resolved, internal water molecules preferentially reside near residues without α-helical and β-sheet secondary structures. These buried waters most often form primary hydrogen bonds to main-chain atoms not involved in intramolecular hydrogen bonds, providing strong evidence that hydrating main-chain atoms is a key structural role of buried water molecules. Additionally, the average B-factor of protein atoms hydrogen-bonded to waters is smaller than that of protein atoms forming intramolecular hydrogen bonds, and the average B-factor of water molecules involved in primary hydrogen bonds with main-chain atoms is smaller than the average B-factor of water molecules involved in secondary hydrogen bonds to protein atoms that form concurrent intramolecular hydrogen bonds. To study the structural coupling between internal waters and buried polar atoms in detail we simulated the dynamics of wild-type FKBP12, in which a buried water, Wat137, forms one side-chain and multiple main-chain hydrogen bonds. We mutated E60, whose side-chain hydrogen bonds with Wat137, to Q, N, S or A, to modulate the multiplicity and geometry of hydrogen bonds to the water. Mutating E60 to a residue that is unable to form a hydrogen bond with Wat137 results in reorientation of the water molecule and leads to a structural readjustment of residues that are both near and distant to the water. We predict that the E60A mutation will result in a significantly reduced affinity of FKBP12 for its ligand FK506. The propensity of internal waters to hydrogen bond to buried polar atoms suggests that ordered water molecules may constitute fundamental structural components of proteins, particularly in regions where α-helical or β-sheet secondary structure is not present. Proteins 2005;60:450–463.** © 2005 Wiley-Liss, Inc.

Key words: buried water; structural coupling; hydrogen bonding; FKBP12

INTRODUCTION

The desolvation of the hydrophobic surfaces of a denatured peptide provides a major driving force behind protein folding.[1,2] The effective "attraction" between hydrophobic side chains leads to the familiar trend that on average nonpolar residues are buried in the core and polar residues are exposed on the surface.[3,4] The presence of polar atoms in the core is, however, unavoidable due to the chemical structure of the peptide bond, which contains an amide nitrogen and a carbonyl oxygen in every repeating unit. A polar atom exposed to the hydrophobic environment incurs an energetic penalty, estimated to be ~ 1–3 kcal/mol based on mutational studies.[5] Nonetheless, polar side chains are common in the core and may be required to achieve stability and fold specificity.[6] The importance of satisfying the hydrogen bonding needs of internal polar groups is clear from the statistical evidence that only a small percentage of buried main-chain NH and CO groups fail to form hydrogen bonds.[7]

Waters in the protein core can promote protein stability by hydrating polar atoms. The stabilizing effects of buried water have been discussed before,[8] and a coupling between the loss of an internal water and local unfolding of the structure has been experimentally observed.[9] Database studies of buried waters have revealed that internal cavities are ubiquitous in globular proteins, some of which contain one or more solvent molecules.[10,11] They have also shown that large cavities in general have a greater probability of containing a solvent,[12] the buried waters on average make three polar contacts with protein atoms,[13] and the solvated cavity surface is more polar than the empty cavity surface and has a higher surface contribution from coil residues.[10] The structural significance of buried water is further highlighted by a recent report that a modified "wet" Hamiltonian that includes a knowledge-based potential to account for long-range water-mediated

Grant sponsor: National Institutes of Health; Grant number: GM 61267

*Correspondence to: Jeffery G. Saven, Department of Chemistry, University of Pennsylvania, 231 South 34th Street, Philadelphia, PA 19104. E-mail: saven@sas.upenn.edu

Received 13 October 2004; Revised 13 January 2005; Accepted 4 February 2005

Published online 3 June 2005 in Wiley InterScience (www.interscience.wiley.com). DOI: 10.1002/prot.20511

interactions improves the efficiency and accuracy of structure prediction for α-helical proteins.[14,15]

While the structural roles of buried waters are well recognized, a statistical study of the structural impact of a buried water on its immediate surrounding has not been reported. To identify the unique features that distinguish interactions of buried waters with neighboring protein atoms, we examined 842 high-resolution structures and characterized the hydrogen bonding patterns of buried water molecules based on the secondary structure and the hydrogen-bonding status of protein atoms. We show that well-resolved, buried water molecules preferentially reside near regions without secondary structure and form hydrogen bonds with main-chain atoms that are otherwise not hydrogen-bonded, whereas the majority of polar side chains that are hydrogen-bonded to buried waters also form intramolecular hydrogen bonds. In addition, we show that the B-factors of water molecules and polar atoms both depend on their hydrogen-bonding partners, resulting in a lower average B-factor for protein atoms hydrogen-bonded to buried waters. Together, these observations provide direct evidence that buried waters and the surrounding polar atoms may be structurally coupled.

To characterize the structural coupling between buried water and protein structure suggested by our database study and to better understand the factors that contribute to a stable protein–water interaction, we performed a molecular dynamics (MD) simulation of a small globular protein FKBP12, which contains an ordered, buried water that forms hydrogen bonds with main-chain and side-chain atoms. We similarly simulated the dynamics of single point mutants of FKBP12 designed to perturb the arrangement of hydrogen bonds around the water. A comparative analysis of their dynamics shows a link between the structural water and the local protein conformation that depends on the orientation of the water molecule. Since some of the observed structural changes are likely to interfere with the binding of a ligand such as FK506, these findings suggest that a functional assay measuring the affinity for FK506 may be an efficient readout for probing the conformational changes resulting from modified hydrogen bonds to the conserved water.

METHODS

Identification of Hydrogen Bonds

For the purpose of this study, the following simplifications were made regarding the hydrogen-bonding potential of polar atoms. All nitrogens are considered potential hydrogen-bond donors; carbonyl oxygens and Asp and Glu side chains are considered potential hydrogen-bond acceptors. The hydroxyl group of Ser, Thr, and Tyr are considered hydrogen-bond donors because the hydrogen-bonding criteria used for protein donors and protein acceptors result in comparable coverage of the conformational space when the hydroxyl groups are considered hydrogen-bond acceptors. McDonald and Thornton[7] also noted that a high percentage of side-chain hydroxyls fail to accept hydrogen bonds due to steric crowding. Cys sulfurs are hydrogen-bond donors.

For donor atoms, the position of a hydrogen was determined based on geometrical considerations. For donors (D) attached to two heavy atoms (DD1 and DD2), such as amide nitrogens and nitrogens of His and Trp side chains, a hydrogen was placed 1 Å away from the donor atom bisecting the angle formed by DD1-D-DD2, so that the hydrogen lies in the same plane as the three heavy atoms. For donors attached to a single heavy atom (DD), the placement of hydrogen varied depending on the hybridization state. For *sp2* hybridized donors, such as amides of Asn, Gln, and Arg side chains or the hydroxyl of Tyr, a hydrogen was placed in each of the two possible positions: 1 Å from the donor D with the DD-D-H angle of 120° (nitrogen) or 110° (oxygen) in the plane of the heavy atoms D, DD, and DDD (an atom two covalent bonds from the donor). For *sp3* hybridized donors, that is, the terminal amine of the peptide main chain or Lys side chain, the hydroxyl of Ser and Thr, and the sulfhydryl of Cys, a hydrogen was placed 1 Å away from the donor at a constant DD-D-H angle of 96° (sulfur), 110° (oxygen) and 120° (nitrogen) in the plane of DD, D and the acceptor water molecule.

Two sets of geometric criteria were used to determine if a hydrogen bond exists between a buried water molecule and a protein atom: (1) for hydrogen bonds between protein donors and water acceptors, a hydrogen bond was declared if the water molecule (W) exists within 2.5 Å of the donor hydrogen and makes an angle W-H-D $> 90°$; (2) for hydrogen bonds between protein acceptors and water donors, a hydrogen bond was declared if the water exists within 3.3 Å of the acceptor atom A and makes an angle W-A-AA $> 80°$, where AA is the heavy atom that A is attached to. No hydrogen bond was allowed to the amide of proline. The more permissive angle cutoff used in (2) accounts for the water hydrogen, which is not visible in the structure and is therefore allowed to rotate freely about the water oxygen to adopt the best hydrogen-bonding geometry. These cutoffs were optimized to include the major peak of each distance-angle distribution (see also McDonald and Thornton[7]). Because the hydrogen-bond distance and angle distributions each have a clear major peak, the conclusions from this study do not change qualitatively when different cutoff values are used (data not shown).

Molecular Dynamics Simulation

NAMD2[16] with the all atom force field CHARMM (v. 27)[17] was used to simulate FKBP12 (PDB 1D6O chain A) and the E60 mutants. The protein was immersed in a water box filled with modified TIP3 molecules, with > 8 Å of water separating protein atoms and the nearest surface of the solvent box. Sodium and chloride ions were added to achieve charge neutrality and an ionic strength of 50 mM. Prior to the dynamic simulation, protein and water molecules were energy-minimized for 1000 steps using the steepest-descent method, after which the total energy of the system was nearly invariant upon further minimization. The temperature was then gradually increased to 300 K in increments of 1 K over 6 psec. The simulation was

continued for another 12 ns in 1.5 fs time steps under constant pressure (1 atm) and temperature (NPT) using periodic boundary conditions. All bonds connecting hydrogens and heavy atoms were held rigid. The electrostatic interactions were implemented using the particle mesh Ewald method with 1 Å grid spacing. Nonbonded forces were gradually switched off between 10–12 Å and the pair list was updated every 10 steps (every 15 fs). Structures were saved every 0.75 ps for analysis, resulting in 16,000 structures per simulation. The RMSD was evaluated by least square fitting the backbone heavy atoms (N, CA, C, O) of energy minimized and simulated structures. The individual residue RMSD's and hydrogen bonding statistics were evaluated over the period of 1.5–12 ns.

RESULTS

Distribution of Buried Hydrogen Bonds

We characterized the hydrogen bonds between buried water molecules and core polar atoms by analyzing 842 high resolution ($\leq$ 1.7 Å) nonredundant globular structures to study the relationship between internal waters and their neighboring polar atoms. (The list was obtained from http://dunbrack.fccc.edu/bbdep/bbdep02.May.cmpdlist.gz.) Buried water molecules were identified by computing the solvent-accessible surface area (ASA) of every nonhydrogen atom in each structure using NACCESS.[18] Based on the calculation, those water molecules that are accessible to a probe of 1.4 Å radius rolling on the surface[19] were iteratively removed from the structure until all remaining waters had zero ASA. A polar atom was similarly classified as a core atom if its ASA is less than 5% of the maximum value observed for its atom type among all structures (Table I). These requirements on water molecules and polar atoms ensure that only hydrogen bonds formed within the protein core are included in the current study. The hydrogen bond between a buried water and a core polar atom was identified based on geometrical considerations (see Methods and McDonald and Thorton[7]).

In total, we observed 6718 buried water molecules engaged in 15,177 hydrogen bonds (Table II). As one might expect for buried solvent, a large percentage (78%) of these waters make two or more hydrogen bonds to the protein, and the distribution of the hydrogen bond multiplicity m between buried water molecules and core protein atoms shows a peak at $m = 2$ [Fig. 1(a)]. Since buried waters are likely to form multiple hydrogen bonds with neighboring atoms, and also because water molecules forming multiple hydrogen bonds are likely to be structurally more important, we required $m \geq 2$ for the current analysis (also, see Rashin et al.[12] where $m \geq 3$ was used to define buried waters). In computing the multiplicity, we did not consider water–water interactions since the focus of this study involves the distribution of buried waters with respect to the local protein environment rather than identifying water clusters.[11] The total number of buried waters (N_w) increased with protein size (N_r) as $N_w = \alpha(N_r^{1/3} - \beta)^3$ (see Janin[20]), where $\alpha = 0.249$ and $\beta = 3.15$ are fitted constants, suggesting that most of the waters included in the analysis are structural waters [Fig. 1(b)].

TABLE I. The Maximum ASA Observed for Different Polar Atoms

Residue	Atom	ASA_{max} (Å^2)
Ala	N	55.4
	O	47.1
Cys	N	43.8
	O	35.0
Asp	N	51.6
	O	44.7
	OD1/2	59.5
Glu	N	54.7
	O	37.8
	OE1/2	66.7
Phe	N	52.4
	O	38.1
Gly	N	57.4
	O	46.3
His	N	42.0
	O	35.1
	ND1	30.3
	NE2	40.8
Ile	N	50.1
	O	39.8
Lys	N	48.8
	O	41.0
	NZ	81.9
Leu	N	54.6
	O	38.2
Met	N	47.6
	O	35.2
Asn	N	45.8
	O	39.5
	ND2	71.2
	OD1	40.2
Pro	N	22.8
	O	40.8
Gln	N	46.2
	O	39.5
	NE2	71.3
	OE1	41.1
Arg	N	53.8
	O	35.7
	NE	56.8
	NH1/2	74.1
Ser	N	48.0
	O	39.3
	OG	63.0
Thr	N	52.8
	O	40.4
	OG1	44.7
Val	N	45.9
	O	33.2
Trp	N	39.1
	O	37.2
	NE1	37.0
Tyr	N	39.1
	O	37.2
	OH	68.5

We plotted the distribution of water hydrogen bonds involving different secondary structures in the protein core (Fig. 2). Buried waters are unevenly distributed in the protein core, with a threefold to fivefold greater propensity

TABLE II. The Distribution of Buried Water Molecules by Secondary Structure and Multiplicity

	$m = 1$	2	3	4	5	6	Sum
Secondary structure							
B	12	82	125	51	7	0	277
E	324	1177	1373	478	75	4	3431
G	61	230	256	87	21	4	659
H	407	1149	898	271	33	1	2759
I	0	1	0	0	0	0	1
S	142	613	774	315	58	5	1907
T	137	552	596	183	28	0	1496
U	389	1556	1960	619	113	10	4647
Number H-bond	1472	5360	5982	2004	335	24	15177
Number water	1472	2680	1994	501	67	4	6718

The secondary structure notation: B, isolated β-bridge; E, extended strand; G, 3-helix; H, α-helix; I, 5-helix; S, bend; T, hydrogen-bonded turn; U, undefined.

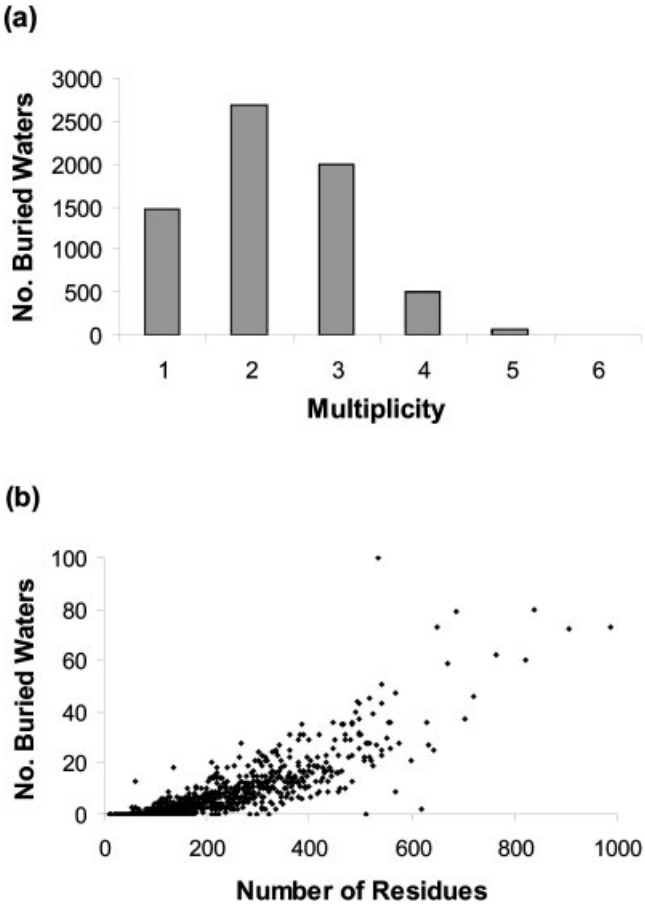

Fig. 1. **a:** The hydrogen bonding multiplicity of buried water molecules. Here, multiplicity refers to the total number of polar contacts satisfying the distance and angle criteria (see Methods). **b:** The number of buried waters is a function of the protein size.

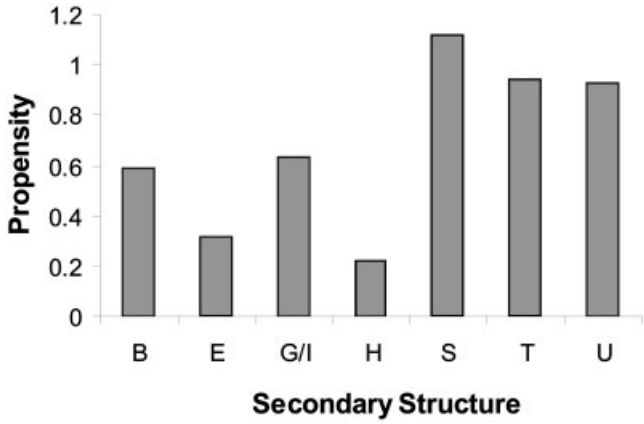

Fig. 2. The hydrogen bond propensity for different structural elements was obtained as the ratio of the conditional probability that a buried water is hydrogen-bonded to a particular secondary structure, p_{hbond} (sec struct), with the probability of each secondary structure, p(sec struct), in the protein core, i.e., $\frac{p_{hbond}(\text{sec struct})}{p(\text{sec struct})} = \left(\frac{N_{hbond}(\text{sec struct})}{\sum_{\text{sec struct}} N_{hbond}(\text{sec struct})}\right) / \left(\frac{N(\text{sec struct})}{\sum_{\text{sec struct}} N(\text{sec struct})}\right)$. The secondary structure notation from NACCESS[18] signifies: B, isolated β-bridge; E, extended strand; G, 3-helix; H, α-helix; I, 5-helix; S, bend; T, hydrogen-bonded turn; U, undefined. G and I were combined together due to the limited statistics for I.

of appearance near residues in turns and coils (S, T, U) compared to residues in α-helices (H) or β-sheets (E). We then computed the average number of hydrogen bonds from each water to main-chain and side-chain atoms for each secondary structural element. Regardless of the local secondary structure, there are more hydrogen bonds to main-chain atoms than to side-chain atoms [Fig. 3(a)]. This bias reflects the usual hydrophobic nature of buried residues, each of which has two polar atoms in the main chain (except for proline, whose amide nitrogen does not participate in a hydrogen bond) but usually few polar side-chain atoms.

Since a polar atom can simultaneously form multiple hydrogen bonds, we examined whether the distribution of water hydrogen bonds changes when parameterized by the hydrogen bonding status of the protein atom. We thus classified all hydrogen bonds between water and protein as either primary or secondary, depending on whether the protein atom participates in an intramolecular hydrogen bond (secondary) or not (primary). On average the majority of water hydrogen bonds to main-chain atoms are primary [Fig 3(b)]. Interestingly, the relative abundance of primary and secondary hydrogen bonds (p/s) varies with secondary structure. The p/s ratio ranges between 2.2–3.5 for residues without regular secondary structure (B, G/I, S,

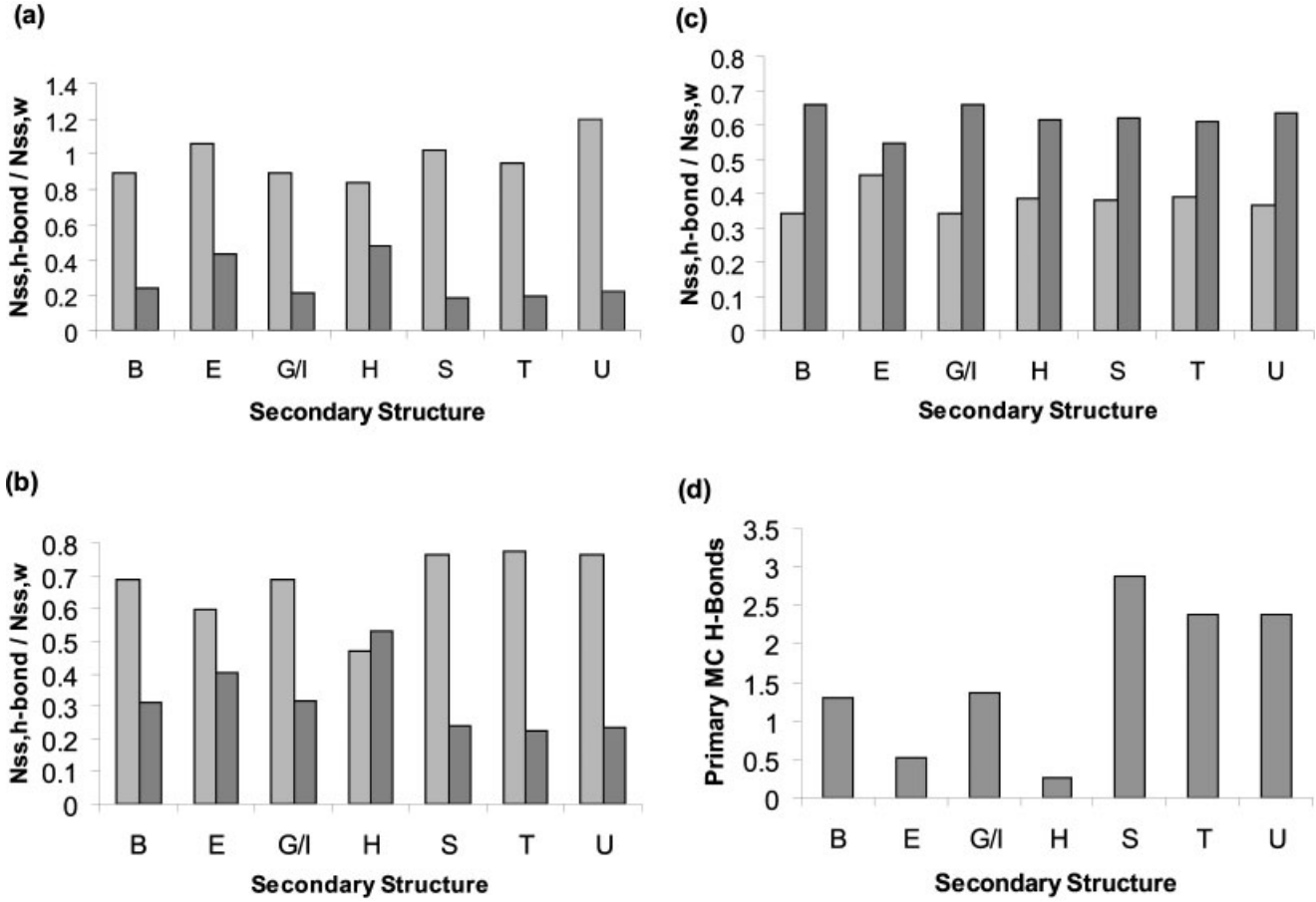

Fig. 3. **a:** The average number of hydrogen bonds per buried water to a particular secondary structures: $N_{ss,H}/ N_{ss,w}$, where $N_{ss,H}$ is the number of water hydrogen bonds involving residues in secondary structure ss, and $N_{ss,H}$ is the number of unique water molecules hydrogen-bonded to the same secondary structure. Main-chain atoms only (light), side-chain atoms only (dark). **b:** The average number of hydrogen bonds per buried water to main-chain atoms that are primary (light) or secondary (dark). **c:** The same as (b) but for side-chain atoms. **d:** The average number of primary hydrogen bonds to main-chain atoms per buried water.

T, U), whereas for residues with secondary structure the ratio is between 0.9–1.5 (E, H). In contrast to main-chain atoms, side-chain atoms have primary to secondary hydrogen-bond ratio of $p/s = 0.5 - 0.8$ independent of the secondary structure, suggesting that hydrogen bonds between water and side-chain atoms are largely insensitive to the underlying local structure [Fig. 3(c)]. The observed dependence of main-chain p/s on secondary structure suggests that the hydrogen-bonding potential of main-chain atoms outside α-helices and β-sheets remains largely unfulfilled [Fig. 3(d)]. Buried waters appear to perform the task of satisfying the unmet hydrogen-bonding needs of main-chain polar atoms in unstructured regions of the protein core.

The crystallographic temperature factor (B-factor) reports on the quality of the electron density obtained in X-ray diffraction and correlates with the mobility of an atom around the local minimum. In general, the B-factor decreases with improved structural resolution since each atom is on average better localized in the structure. We compared the temperature factors of buried waters and protein atoms involved in hydrogen bonds to see what factors contribute to their variation. The average B-factor of buried water molecules decreases with the number of hydrogen bonds up to $m = 3$ [Fig. 4(a)], suggesting that each additional hydrogen bond helps immobilize the water. On the other hand, additional hydrogen bonds beyond the first three appear to have little effect on the measured B-factors. A similar trend is observed when the B-factors are plotted separately for main-chain and side-chain hydrogen bonds [Fig. 4(b,c)]. We repeated the analysis using only the structures with resolutions between 1.5–1.7 Å to see whether there is a systematic bias due to crystallographic resolution. That we obtain the same qualitative conclusions shows that these differences reflect structural correlations and not statistical artifacts (data not shown).

A structural coupling between buried waters and the polar atoms around them may result in an observable correlation in their temperature factors. To that end, we computed for each secondary structure the average B-factor of water molecules forming either primary or secondary hydrogen bonds. Independent of the secondary structure the water molecules involved in primary hydrogen bonds to the backbone consistently have a lower temperature factors than those forming secondary hydrogen bonds [Fig. 5(a)]. However, the difference between the primary and secondary

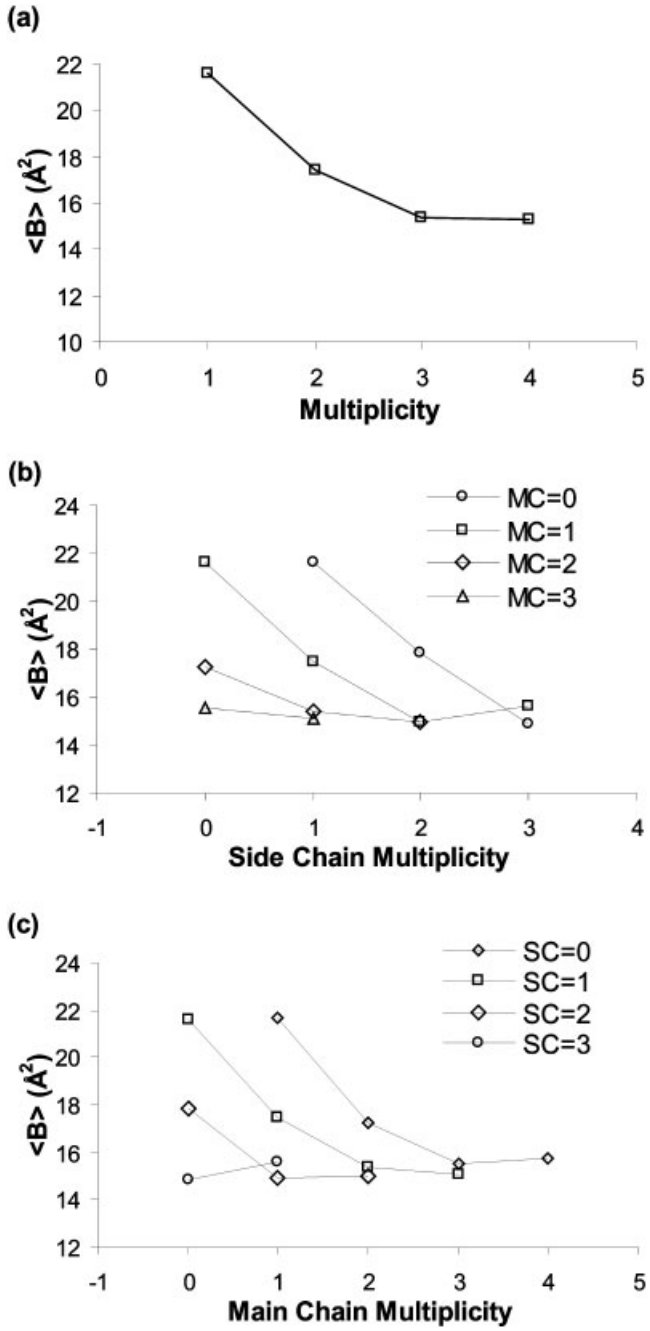

Fig. 4. **a:** The average B-factor of buried waters as a function of the hydrogen-bond multiplicity. **b:** The average B-factor of buried waters was plotted as a function of the number of hydrogen bonds to side-chain atoms. The number of hydrogen bonds to main-chain atoms is constant for each curve. **c:** The average B-factor of buried waters was plotted as a function of the number of hydrogen bonds to main-chain atoms. The number of hydrogen bonds to side-chain atoms is constant for each curve.

hydrogen bonds exists only for main-chain atoms and is absent for side-chain atoms [Fig. 5(b)]. We also plotted the average B-factor of buried polar atoms in each secondary structure to see how their mobility is affected by the types of hydrogen bonds they form. For both main-chain and side-chain atoms, the average B-factor is smaller when they form intermolecular hydrogen bonds with buried waters than when they form intramolecular hydrogen bonds with other protein atoms [Fig. 5(c,d)]. Interestingly, the protein atoms appear to be more immobilized (lower B-factor) when hydrogen bonding to internal water than when forming an intramolecular hydrogen bond.

Simulation of FKBP12

Since a water that forms multiple hydrogen bonds to main-chain atoms is likely to be structurally important, its loss is expected to have a measurable impact on the stability, folding, and function of a protein. Studying the response of a protein to a mutation that perturbs a conserved water may thus help elucidate its structural role and characterize the structural coupling between buried water and protein structure suggested by the database study. To monitor the time-dependent movement of a water as well as the corresponding protein response in atomic detail, we performed a molecular dynamics (MD) simulation of a small globular protein FKBP12 and its single point mutants. FKBP12 is a 107-residue peptidyl-prolyl isomerase that has been well conserved during evolution. The protein, which binds a class of immunosuppressants including FK506 and rapamycin,[21] has been the target of biochemical and mutational studies.[22–24] The apo and ligand-bound structures of FKBP12 have been solved by crystallography and NMR,[25–27] and show a water molecule Wat137 lodged near the loop connecting β4 with the only α-helix [Fig. 6(a,b)]. Hydrogen bonds to main-chain atoms of residues M49, Q53, and E54 and a hydrogen bond to the E60 side chain place Wat137 at the center of a tetrahedral coordination.

High resolution structures of FKBP12 suggest that the E60 side chain may play a key role in orienting and stabilizing Wat137. If true, it may be possible to alter the interaction between Wat137 and the nearby 50s loop (residues 49 to 56—nomenclature according to Liang et al.[28]) by substituting E60 with an amino acid that is unable to hydrogen-bond with the water. To test this possibility, we performed 12-ns molecular dynamics simulations of wild type FKBP12 and four mutants containing a substitution at E60: E60A, E60Q, E60S and E60N. We also simulated the dynamics of wild type without the water molecule (wtNW) to directly examine the structural contribution of Wat137. The mutations chosen in this study should not affect the stability or the fold of the protein significantly since E60 is located on the solvent-accessible surface of an α helix. There is also experimental evidence by circular dichroism spectroscopy that the E60A mutation does not significantly affect the secondary structural content of the protein.[29]

The residue-specific RMS deviation (RMSD) calculated by averaging the individual amino acid RMSD during 1.5–12 ns of simulation shows differences in the 50s loop [Fig. 7(a)]. The Ramachandran plots of wild type shows that K52 adopts ϕ-ψ angles corresponding to an α-helix and Q53 adopts a conformation typical of a left-handed helix [Fig. 7(b)], whereas the same residues in the E60A mutant both adopt an extended conformation [Fig. 7(c)]. A

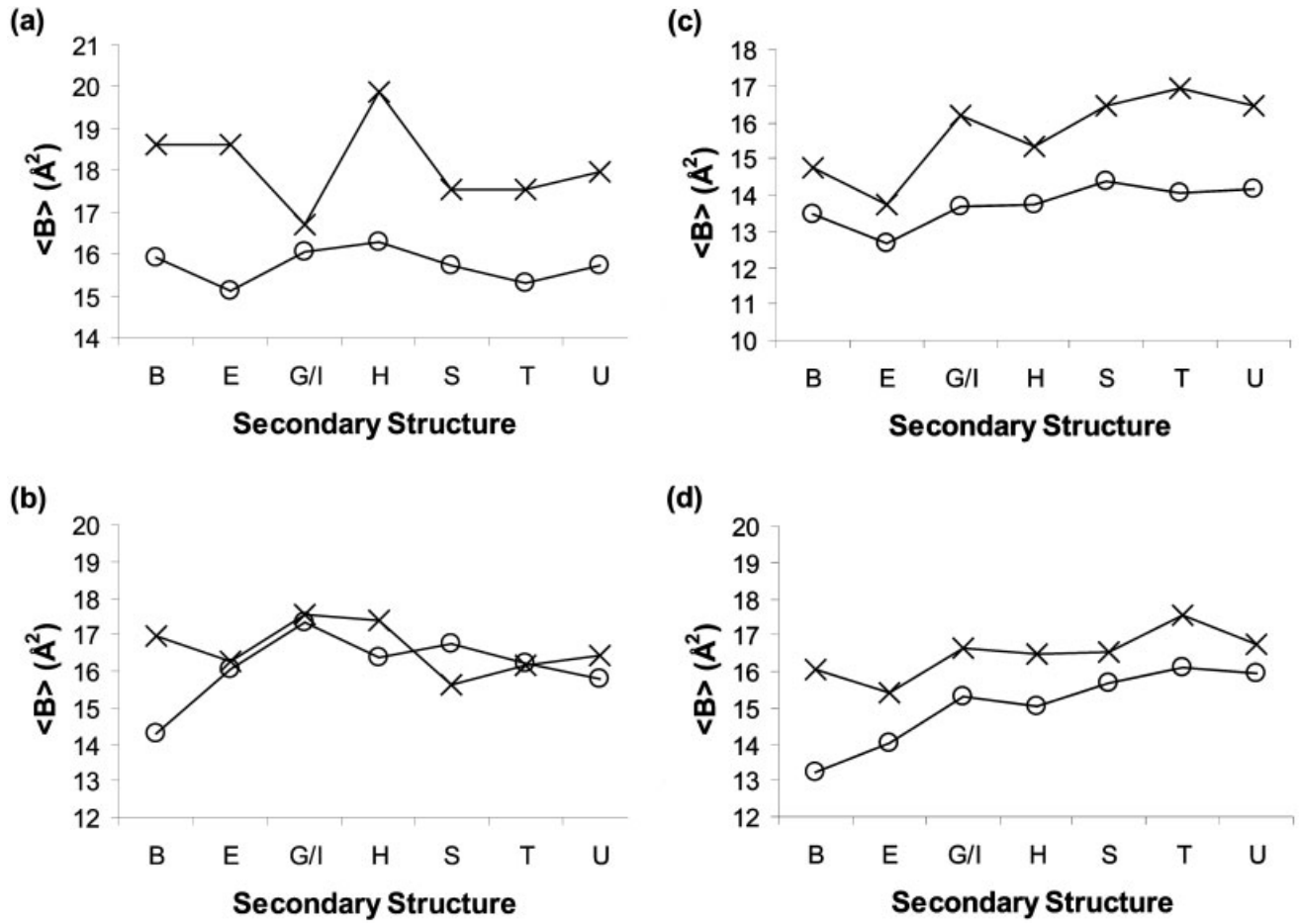

Fig. 5. **a:** The average B-factor of buried waters making primary (—○—) and secondary (—×—) hydrogen bonds to main-chain atoms. **b:** The average B-factor of buried waters making primary (—○—) and secondary (—×—) hydrogen bonds to side-chain atoms. **c:** The average B-factor of main-chain atoms hydrogen-bonded to water alone (—○—) and other protein atoms alone (—×—). **d:** The average B-factor of side-chain atoms hydrogen-bonded to water alone (—○—) and other protein atoms alone (—×—).

similar rearrangement of the main-chain dihedrals is observed for E60Q, which is unable to form a stable hydrogen bond with the water, but not for E60S or E60N, for which the hydrogen bond between Wat137 and the side chain is mediated by another water molecule. The 50s loop, however, undergoes the same rearrangement in E60N after Wat137 escapes into the solvent. During the simulation of wtNW, two water molecules from the bulk solvent sequentially enter the vacant space of Wat137 (during 5.2–9.0 ns and 9.7–12 ns of simulation), partially restoring the network of hydrogen bonds observed for wild type. The local conformation of the 50s loop in wtNW remains close to that of wild type (data not shown).

The curved β sheet of FKBP12 wraps around the lone α-helix, creating a ligand-binding pocket comprising residues from the α-helix and the final two strands of the sheet. Although these two regions are sequentially distant, van der Waals interactions and hydrogen bonds keep them spatially close. The hydrogen bond between G58 NH and Y80 CO bridges the amino terminus of the helix with residues from the 80s loop, and may be important in maintaining a functional binding pocket. We plotted the distance between G58 NH and Y80 CO to quantify how the effects of localized protein–water interactions propagate to the rest of the protein. For wild type, as well as for E60S and E60Q, the interatomic distance remains close to an average of 2.1 Å throughout the simulation, indicative of a persistent hydrogen bond [Fig. 8(a)]. Similarly, the hydrogen bond remained intact during a repeated 12-ns simulation of wild type (data not shown). In contrast, the corresponding hydrogen bond is rapidly lost during the simulation of E60A and E60N [Fig. 8(b)], resulting in a regional shift of the 80s loop away from the ligand binding pocket. Interestingly, the hydrogen bond that is absent during the early part of the simulation of wtNW is restored at ~ 10.5 ns, shortly after the appearance of a long-lived water (residence time > 2.3 ns) near the 50s loop at 9.7 nsec. In support of the hypothesis that the loss of the hydrogen bond is coupled with the loss of a structural water, we observe both a stable hydrogen bond and a residence time > 12 ns for Wat137 during the second 12 ns simulation of E60A (data not shown). However, the loss of the G58 NH–Y80 CO hydrogen bond in E60N despite the long residence time of Wat137 shows the correlation is not

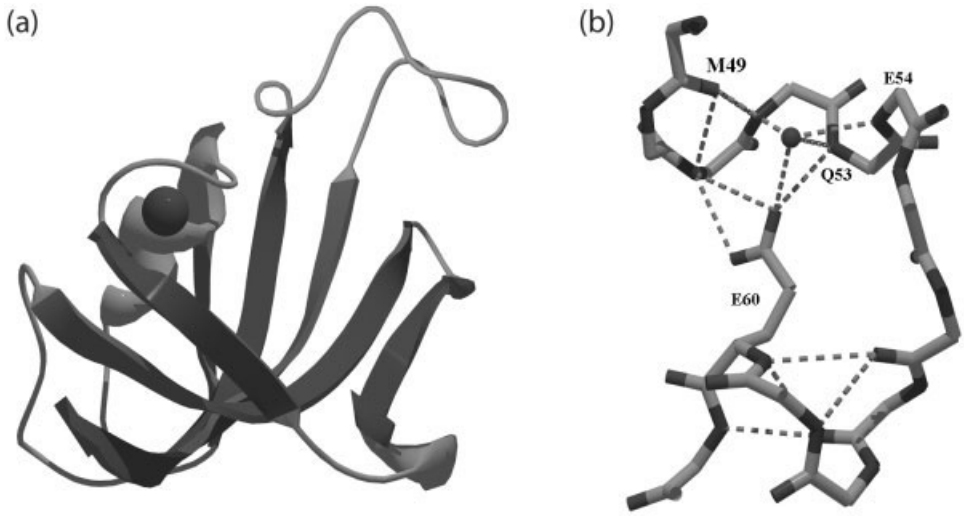

Fig. 6. **a:** A rendering of FKBP12 with Wat137 represented as a sphere (from PDB: 1FKF). **b:** The hydrogen-bond network around Wat137 showing the solvent molecule coordinating hydrogen bonds between main-chain atoms and E60 side chain. Figures were generated using Swiss PDB-Viewer [65] and POV-Ray v3.5.

perfect, suggesting there are other effects coming from the point mutation.

The indole ring of W59 forms the basin of the binding pocket and contributes to ligand binding through van der Waals interactions.[29] While the residue is oriented perpendicular to the axis of the helix in the solution and crystal structures of FKBP12 [Fig. 9(a)], the side chain often populates a different rotamer state during the simulation [Fig. 9(b)]. However, the second rotamer state is observed with different likelihood for wild type and mutants, suggesting that structural changes near residue 60 may be responsible for this side-chain rotation. The frequency of hydrogen bond, $f_{60CO\text{-}64NH}$, between residues 60 and 64 is significantly higher in the simulated structures of E60A compared to wild type (93% occupancy in E60A vs. 63% in wild type), and correlates with the change in the χ_1 dihedral angle of W59. The formation of hydrogen bond to residue 60 is in turn lower when the side chain of residue 60 is either directly or indirectly involved in a stable hydrogen bond to Wat137 than when the side chain is either unable to interact with the water, for example, E60A, or the interaction is weak, for example, E60Q (Fig. 10). The main-chain hydrogen bond to residue 60 removes a bulge in the helix that is conserved in FKBP12 and a related protein FKBP12.6,[29] and in so doing appears to favor the alternate conformation of W59 observed during the simulation. Therefore, Wat137 determines not only the local conformation of the 50s loop through direct hydrogen bonds, but also influences the preferred side-chain conformation of W59 by affecting the formation of a main-chain hydrogen bond in the helix. The steric clash between the new conformation of W59 and a bound ligand should result in reduced affinity of E60A for FK506. Our simulations thus predict that the disorientation of an ordered water, as observed in the E60A and E60Q mutants of FKBP12, will lead to a combination of structural changes, which may be indirectly probed in a ligand-binding assay.

DISCUSSION

While globular proteins often bury hydrophobic residues in the core and expose polar residues on the surface, this binary patterning has many exceptions. Buried polar side chains may play a key role in ensuring a unique protein topology[30] although this often incurs a penalty in protein stability or the folding kinetics.[31,32] Buried water molecules often participate in enzymatic reactions,[33–35] interdomain motion,[36] ligand recognition,[37] and the solvation of buried polar atoms.[38,39] The database and structural studies to date strongly suggest integral roles of buried waters in different protein topologies, where they are thought to promote protein stability by hydrating polar atoms. [10,11,38–41] The energetic contribution of buried solvent molecules is supported by the structural destabilization of cavity creating mutations.[42] Site-directed mutations that bury polar atoms similarly destabilize the structure.[5]

Although buried water molecules have been studied in detail in system-specific ways,[40,41] a complete understanding of the behavior of buried solvents is still lacking. A systematic experimental study of buried water molecules must cope with many factors that are highly context dependent. For example, cavity creating mutations do not always bury water molecules,[43,44] even when such cavities are sufficiently large to accommodate a solvent molecule. Likewise, substituting a polar residue that is hydrogen-bonded to a buried water molecule with an isosteric nonpolar residue does not predictably displace the water.[45] There are examples in which a structural water has been successfully displaced with a single mutation. The T9G mutation in IL-1β removes the water molecule bridging two adjacent β-strands and consequently destabilizes the structure.[46] Similarly, the G36S substitution of BPTI,[47]

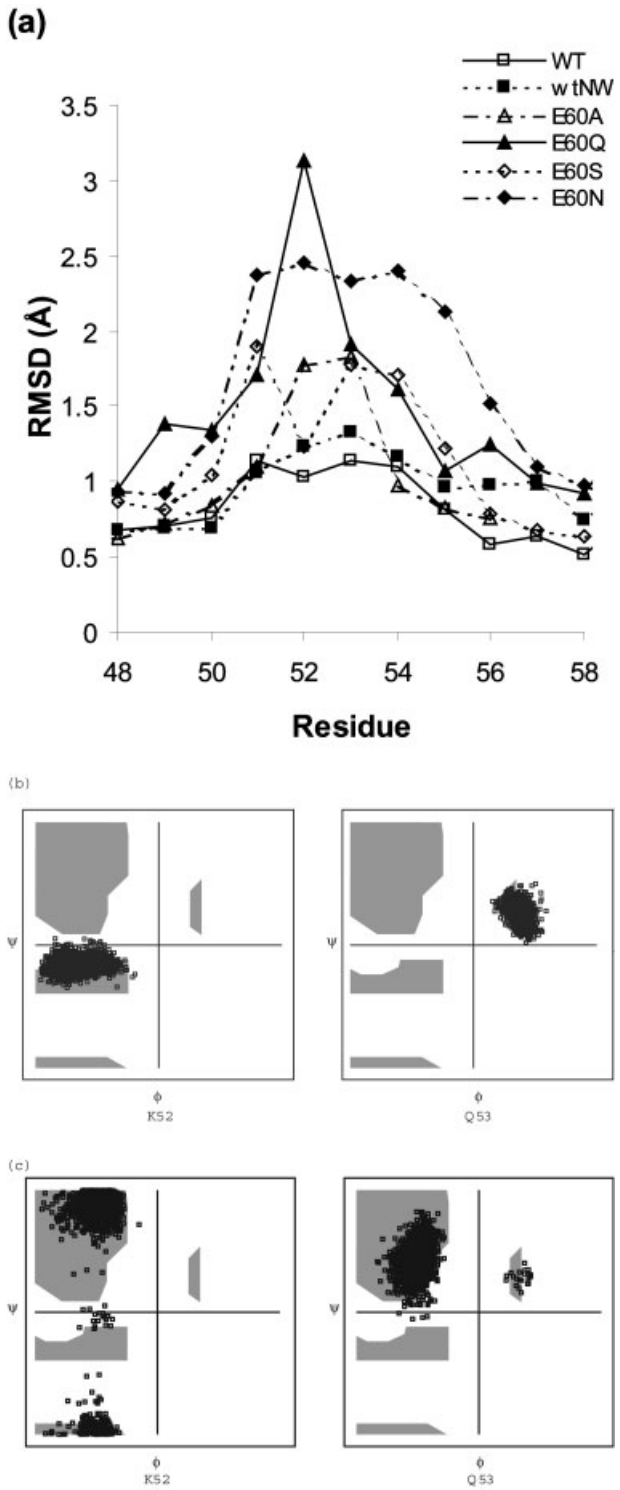

Fig. 7. **a:** The residue-specific RMSD (Å) of wild-type and mutant FKBP12 during 1.5–12 ns of simulation. The simulation of wild type was repeated without Wat137 (wtNW). **b:** The Ramachandran plots of K52 and Q53 for wild type during the simulation. **c:** Similarly for E60A.

the N52I mutation of Iso-1-cytochrome c,[48] and hydrophobic mutations of H64 of sperm whale myoglobin[49] have all resulted in loss of a structural water. Yet, these examples do not provide a general strategy of constructing targeted mutants with modulated protein–water interactions, which is required to generate a large number of mutants with subtly varying protein–water interactions for comparative study. The T152 → A,S,C,V,I mutations of T4 lysozyme fail to displace the buried solvent as expected but simply move it by up to 1.7 Å,[45] illustrating our limited ability to manipulate buried solvents predictably.

We analyzed a large number of nonhomologous globular proteins to see if buried waters exhibit any distinguishing structural characteristics. Our findings, which are based on comparing water hydrogen bonds, are in qualitative agreement with the observations made based on cavity characterization, i.e., buried water molecules are important in solvating polar atoms.[38–40] An analysis of internal cavities in 121 structures by Hubbard et al.,[10] for example, showed that empty cavities often contain nonpolar side chains with secondary structure whereas solvated cavities possess a more polar surface and include a large contribution from main-chain atoms. We similarly observe that buried waters appear preferentially near regions without secondary structure, e.g., loops and turns, and the majority of these waters make primary hydrogen bonds to main-chain atoms. However, because our dataset is much larger we were able to perform new correlation studies by further parameterizing water hydrogen bonds with variables that have not been used in the past for similar studies. Accordingly, the normalized probability of primary hydrogen bond to main-chain atoms is seen to vary by as much as 11-fold between α-helix and "bend" [Fig. 3(d)], whereas the contribution to solvated cavity surface from coil residues was previously determined to be only 1.6–2.8 times greater than from residues with secondary structure (Table IV in Hubbard et al.[10]). Residues outside α-helix and β-sheet secondary structures are far more likely to hydrogen-bond with buried waters than residues in these canonical secondary structures.

It has been reported that there are more water hydrogen bonds to main-chain carbonyls than to amides.[10,11] Here we provide a rational explanation for this bias by examining primary and secondary hydrogen bonds separately. We note that buried waters are on average 39 times more likely to form a secondary hydrogen bond to a carbonyl oxygen than to an amide nitrogen. The secondary hydrogen bonds occur more often with carbonyl oxygens because a carbonyl oxygen can simultaneously form two hydrogen bonds, whereas an amide nitrogen can typically form only one hydrogen bond at a time. In contrast, this excess is only 1.3 times when the statistics is restricted to primary hydrogen bonds, and steric crowding near an amide nitrogen may account for the residual disparity. The 2.3 excess for main-chain oxygen, which is obtained by averaging all water hydrogen bonds involving backbone atoms, closely resembles the reported approximately twofold difference.[50]

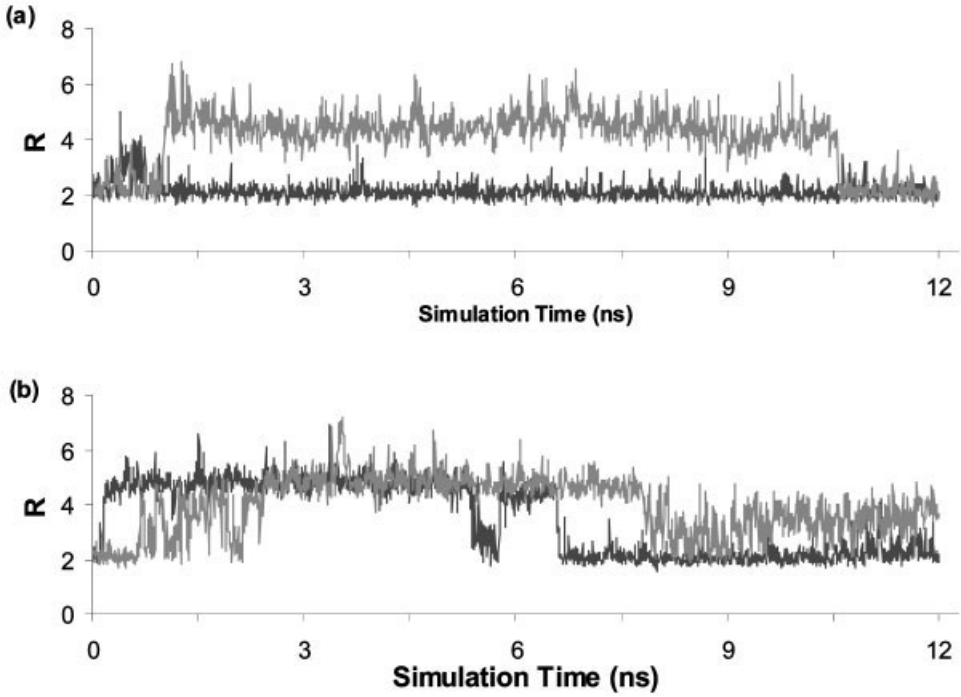

Fig. 8. **a:** The distance *R* between G58 NH and Y80 CO for wild type (dark). The results for E60S and E60Q, not shown for clarity, look identical. The simulation of wild type was repeated without Wat137 (light). **b:** Similarly for E60A (dark) and E60N (light).

Proteins may bury water molecules to ensure internal polar atoms are properly hydrogen-bonded. Being far smaller than a typical amino acid (11.5 $Å^3$ vs. 89 $Å^3$ of Ala), water takes up little volume yet helps stabilize the protein structure by solvating core polar atoms that would otherwise remain without a hydrogen bond. Water can also serve both as hydrogen-bond donor and hydrogen-bond acceptor, forming up to four hydrogen bonds simultaneously. The network of main-chain hydrogen bonds within secondary structural elements makes water hydrogen bonds less probable in the vicinity of α-helices and β-sheets, resulting in the lowest *p*/*s* ratio for α-helices [Fig. 3(b)]. The smaller *p*/*s* ratio for side-chain atoms (0.5–0.8) relative to main-chain atoms (0.9–3.5) implies that side chains often form intramolecular hydrogen bonds and a water hydrogen bond to a side-chain atom is on average less critical than a similar hydrogen bond to a main-chain atom. The lower *p*/*s* ratio of side chains may also reflect the selective pressure on polar side-chain atoms to form hydrogen bonds, since polar side chains not involved in a hydrogen bond are energetically unfavorable and could be replaced with nonpolar residues. To that end, the average numbers of intramolecular hydrogen bonds for buried side chain, 1.5, is greater than that of main-chain atoms, 1.1.

Our study, however, does not exclude the possibility of finding water molecules in a nonpolar environment where they may exist without forming stable hydrogen bonds. Although the protein core often packs hydrophobic side chains with the density of organic solvent,[51] studies have found "packing defects" in the protein interior that are large enough to accommodate one or more water molecules.[12] Using NMR, Ernst et al.[52] have reported the presence of water molecules in a hydrophobic cavity that had previously been declared empty by crystallography. Since the structures we have examined have all been obtained by X-ray diffraction, we may have potentially overlooked the water molecules that do not result in detectable electron density. Our analysis was also based on compiling water hydrogen bonds rather than water molecules themselves. As such, the conclusions of the present work do not pertain to "trapped" waters occupying internal cavities without forming hydrogen bonds, whose structural roles must be addressed separately.

Conserved buried waters may play structural roles similar to amino acids. A comparative study of 30 eukaryotic serine proteases has identified 21 highly conserved waters near conserved residues or main-chain atoms of nonconserved residues,[40] suggesting that these waters may play critical structural roles similar to those of interior amino acids. Structural and bioinformatics studies of fungal and bacterial ribonucleases have similarly shown that waters with low accessible surface area and B-factor tend to be conserved in the crystal structures of evolutionarily related proteins.[41] Here we show that the crystallographic temperature of water varies with the hydrogen-bonding status of the associated polar atom [Fig. 5(a,b)], with "cooler" waters forming more primary hydrogen bonds and "warmer" waters forming more secondary hydrogen bonds. This correlation may signify a difference in the quality or the strength of the two types of hydrogen bonds. On the other hand, the polar atoms hydrogen-bonded to buried waters have on average lower tempera-

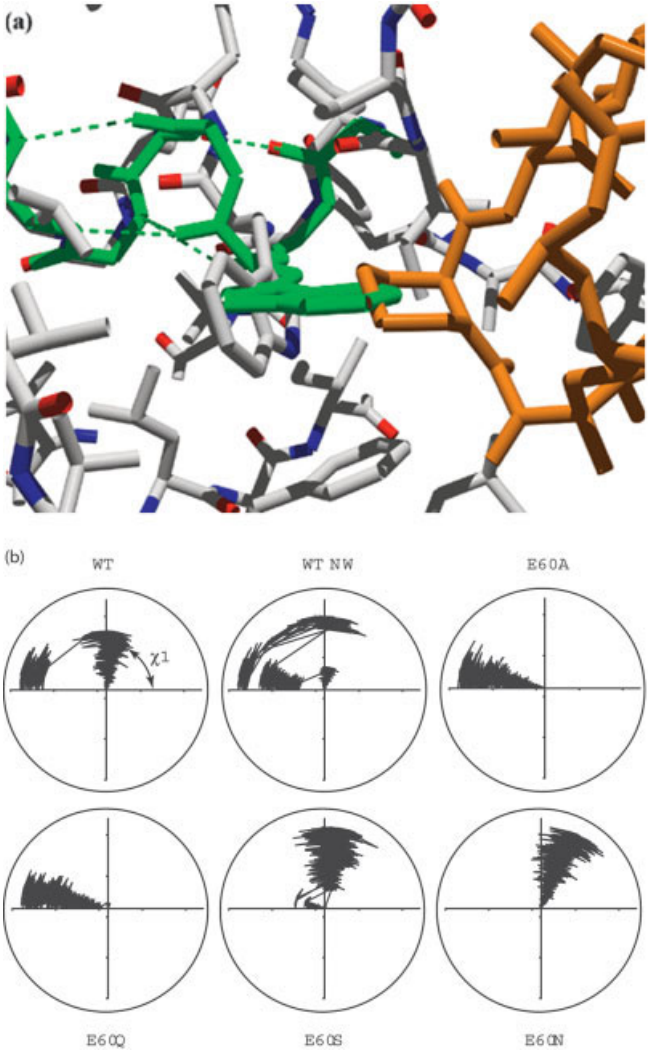

Fig. 9. **a:** The view of FKBP12 around W59 in the presence of a bound ligand FK506 (amber) (from PDB: 1FKF). The alternate rotamer state of W59 observed during the simulation is shown in green. **b:** The $\chi 1$ dihedral angle of W59 during the simulation. Positive $\chi 1$ angles are measured counterclockwise from the positive x-axis. The simulation time is represented by an increasing radius.

ture factors than those forming intramolecular hydrogen bonds [Fig. 5(c,d)], although the average number of intramolecular hydrogen bonds is similar to the average number of intermolecular hydrogen bonds (1.12 and 1.05, respectively). Therefore, a water hydrogen bond is on average more immobilizing for protein atoms than an intramolecular hydrogen bond. Since buried waters are thought to bridge different secondary structural elements,[38,39] the lower temperature factor of protein atoms associated with water may suggest a strong structural coupling of these atoms to the rest of the protein. Given the mutual dependence of structural parameters between buried waters and buried polar atoms, internal solvents may well be viewed as an extension of the protein structure.

The dynamics of protein–water interactions have been studied both experimentally and computationally.[53–55] Since internal waters on average make multiple hydrogen bonds with protein atoms, they are often characterized by long residence times. Denisov et al. have used magnetic relaxation dispersion to directly measure the residence time of Wat122 in BPTI to be 170 ± 20 μs.[57] On the other hand, the typical residence time of hydrating water in the solvation shell does not exceed 200 ps,[58] allowing a meaningful comparison of experimental results with outputs from short MD simulations. MD simulation studies of protein–water interactions have yielded information regarding the structure, dynamics and the mean residence time of hydrating water molecules in and around the protein,[59–61] as well as the chemical potential of cavity waters.[62] In one study, the movement of a buried water molecule in a fatty acid binding protein was simulated as it escapes into the solvent to provide a detailed picture of the interaction between a structural water and the protein.[63]

Although often used to characterize structural waters,[58,63] the residence time alone does not fully characterize their dynamics. In particular, the precise orientation of a water is likely an important parameter since it influences the type and multiplicity of hydrogen bonds formed with the water. The ordering of water molecule within the first hydration shell around a biomacromolecule results in a supramolecular water structure with a net dipole moment that can be observed in simulated structures and may be deduced from cryogenic X-ray structures.[59] The cooperative motions of water molecules around solvated amino acids can also result in a stable dipole-bridge consisting of ordered water dipoles.[64] MD simulations can track the movement and the orientation of a structural water molecule as it interacts with protein in greater detail than experimentally feasible. The simulated dynamics of FKBP12 indicate that Wat137 stabilizes the local loop structure in a manner that depends on its interaction with the side chain of a distant residue. The hydrogen bond between Wat137 and the side chain of E60 ensures that the two lone pairs of the water point to the amides of E54 and V55. Absent this interaction, as in E60A, the water rotates and hydrogen bonds with the K52 carbonyl instead, inducing local conformational changes. Even a conservative mutation such as E60Q facilitates the conformational change by failing to constrain the orientation of Wat137. The inability of Q60 to preferentially hydrogen-bond with the water likely stems from the chemical similarity between the side-chain carbonyl of Q60 and the main-chain carbonyl. In contrast, two other side chains that we have examined, S60 and N60, were more effective in fixing the water in the orientation found in wild type. While their side chains were too short to form a direct hydrogen bond with Wat137, they were assisted by another structural water that effectively increased their radius of influence. In each case, the bridging water had a residence time comparable to that of Wat137, suggesting that it is structurally important. By forming a stable hydrogen-bonded adduct to the polar terminus of S60 and N60, the bridging water may be viewed as extending the covalent structure of the peptide chain to achieve conformational stability.

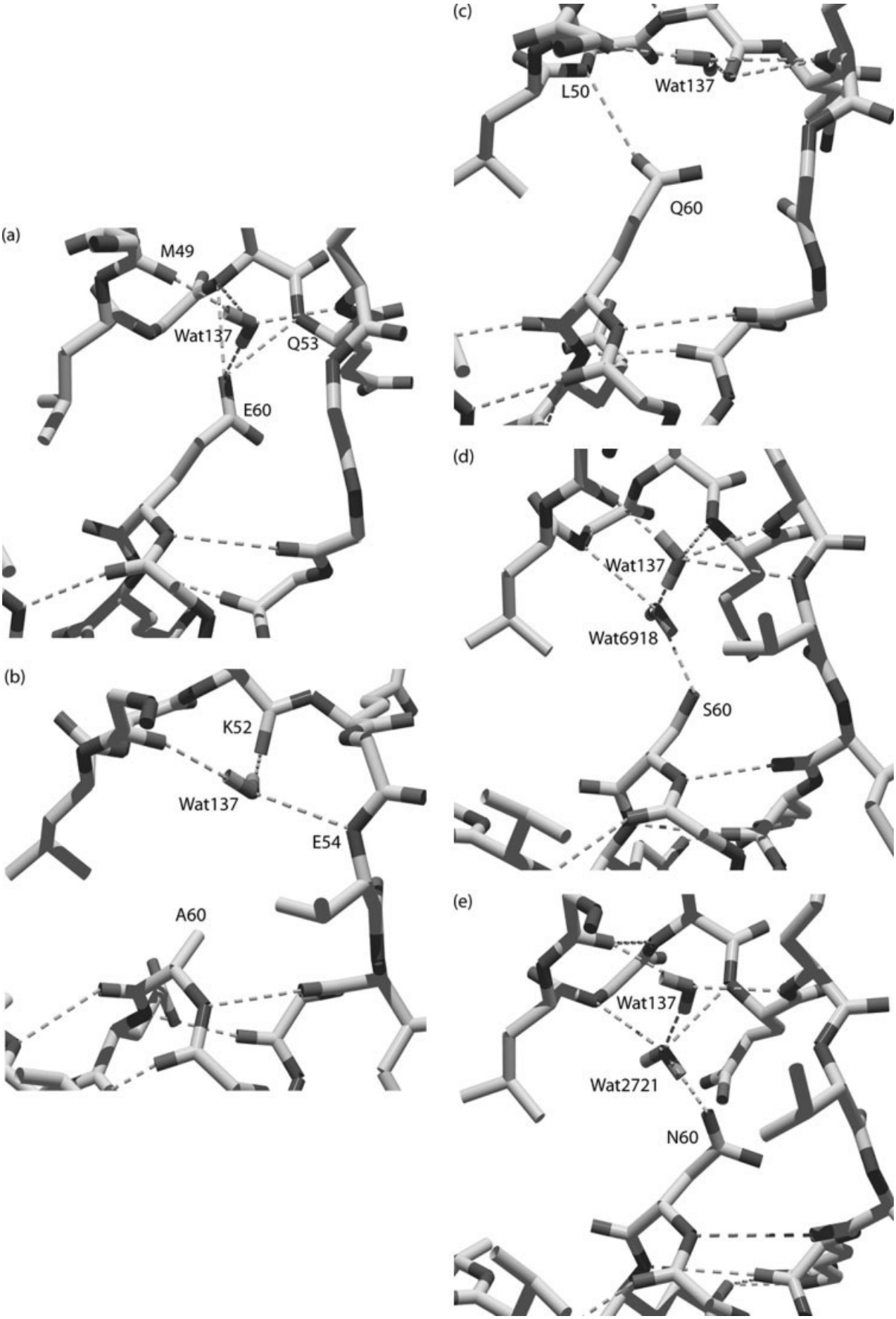

Fig. 10. The network of hydrogen bonds around Wat137 for (**a**) wild type, (**b**) E60A, (**c**) E60Q, (**d**) E60S, (**e**) E60N. The water hydrogen that is not hydrogen-bonded to the carbonyl of M49 rotates up in E60A and E60Q to form a hydrogen bond with K52. In E60S and E60N, bridging water molecules help maintain Wat137 in the same orientation as in wild type.

The conservation of E60 in FKBP12 homologs is suggestive of the importance of maintaining the hydrogen-bonding network around Wat137. In proteins with an E60D substitution, the fully extended side-chain hydrogen bonds with a comparable water molecule (PDB code: 1Q1C), or directly with a main-chain atom in the 50s loop (1PBK, 1KT1). In the protein 1FD9 with an E60T substitution, the helical bulge is created through a direct hydrogen bond between the side-chain amide of Q64 and the T60 carbonyl. Our simulation studies suggest that the loss of the E60-Wat137 interaction may also have functional consequences. First, the hydrogen-bonding frequency to the A64 amide is higher in both E60A and E60Q—two mutants that fail to form a stable hydrogen bond to Wat137. Additionally, the main-chain hydrogen bond to the carbonyl of residue 60 induces a side-chain rotation in W59 that would lead to a steric clash with the bound FK506. While the impact of a bound water on the conformation of nearby loop residues may be expected, it is surprising that a single water seems to provide a key interaction that modulates the rotamer conformation of a distant residue. Although the structure–function relationship surrounding Wat137 is difficult to establish unambiguously, the outcome of the simulations suggests straightforward experimental tests. The functional roles of Wat137 may be investigated by performing a ligand binding assay to probe the conformation of W59, and by determining its structure to confirm the absence of a helical bulge in E60A and E60Q. Validating the predictions from the current study regarding the structure and function of mutant FKBP12s would highlight the importance of characterizing buried waters using both residence time and molecular orientation.

CONCLUSION

We have performed a database analysis of water hydrogen bonds in the protein core and identified several structural characteristics shared by buried water molecules. First, buried waters reside near residues outside α-helices and β-strands where they are important to stabilize residues without secondary structure, largely through hydrogen bonding to their main-chain atoms. This conclusion both confirms and expands upon the findings from previous studies.[10,39] Our study, however, goes beyond characterizing solvated and dry cavities to address the etiology of buried water. We show that the probability of a water hydrogen bond varies with the hydrogen-bonding status of the polar atom, and it is important to distinguish primary and secondary hydrogen bonds when evaluating the interaction of buried waters with protein. Second, a structural coupling between buried waters and the polar atoms gives rise to an observable difference in the temperature distributions, with buried waters and protein atoms they are hydrogen-bonded to each modulating the crystallographic B-factor of the other. A primary hydrogen bond to a main-chain atom lowers the temperature of a water molecule more than a secondary hydrogen bond, whereas the temperature factor of a protein atom is on average lower when it is hydrogen-bonded to a water than to another protein atom. Given that water molecules often bridge distant secondary structures, this implies that these atoms may be more tightly coupled to the rest of the protein, with water serving as "structural glue."

The conclusion from the statistical analysis is supported by simulation studies of wild type and mutant FKBP12. We focused on the structural consequence of perturbing the hydrogen-bonding network around a buried solvent. Point mutants were selected based on their potential to modulate the interaction of Wat137 with its surrounding. We note that the conformations of both near and distant residues are affected by the molecular orientation of Wat137, although the residence time has an effect on the protein dynamics as well. Our study thus suggests that the time-dependent orientation of an internal solvent may be an informative parameter for analyzing protein–water interactions. Given the integral roles of buried waters in protein structure, future protein engineering studies may benefit from considering cavity waters as separate design elements.

ACKNOWLEDGMENTS

The authors acknowledge support from NIH (GM 61267). JGS is a Cottrell Scholar of Research Corporation.

REFERENCES

1. Kauzmann, W. Some factors in the interpretation of protein denaturation. Adv Protein Chem 1959;14:1–63.
2. Dill KA. Dominant forces in protein folding. Biochemistry 1990;29: 7133–7155.
3. Rose GD, Geselowitz AR, Lesser GJ, Lee RH, Zehfus MH. Hydrophobicity of amino acid residues in globular proteins. Science 1985;229:834–838.
4. Miller S, Janin J, Lesk AM, Chothia C. Interior and surface of monomeric proteins. J Mol Biol 1987;196:641–656.
5. Blaber M, Lindstrom JD, Gassner N, Xu J, Heinz DW, Matthews BW. Energetic cost and structural consequences of burying a hydroxyl group within the core of a protein determined from Ala→Ser and Val→Thr substitutions in T4 lysozyme. Biochemistry 1993;32:11363–11373.
6. Bolon DN, Mayo SL. Polar residues in the protein core of Escherichia coli thioredoxin are important for fold specificity. Biochemistry 2001;40:10047–10053.
7. McDonald IK, Thornton JM. Satisfying hydrogen bonding potential in proteins. J Mol Biol 1994;238:777–793.
8. Takano K, Yamagata Y, Yutani K. Buried water molecules contribute to the conformational stability of a protein. Protein Eng 2003;16:5–9.
9. Denisov VP, Halle B. Protein hydration dynamics in aqueous solution: a comparison of bovine pancreatic trypsin inhibitor and ubiquitin by oxygen-17 spin relaxation dispersion. J Mol Biol 1995;245:682–697.
10. Hubbard SJ, Gross KH, Argos P. Intramolecular cavities in globular proteins. Protein Eng 1994;7:613–626.
11. Williams MA, Goodfellow JM, Thornton JM. Buried waters and internal cavities in monomeric proteins. Protein Sci 1994;3:1224–1235.
12. Rashin AA, Iofin M, Honig B. Internal cavities and buried waters in globular proteins. Biochemistry 1986;25:3619–3625.
13. Baker EN, Hubbard RE. Hydrogen bonding in globular proteins. Prog Biophys Mol Biol 1984;44:97–179.
14. Papoian GA, Ulander J, Wolynes PG. Role of water mediated interactions in protein-protein recognition landscapes. J Am Chem Soc 2003;125:9170–9178.
15. Papoian GA, Ulander J, Eastwood MP, Luthey-Schulten Z, Wolynes PG. Water in protein structure prediction. Proc Natl Acad Sci USA 2004;101:3352–3357.
16. Kale L, Skeel R, Bhandarkar M, Brunner R, Gursoy A, Krawetz N, Phillips J, Shinozaki A, Varadarajan K, Schulten K. NAMD2:

greater scalability for parallel molecular dynamics. J Comput Phys 1999;151:283–312.
17. MacKerell AD, Bashford D, Bellott M, Dunbrack RL, Evanseck JD, Field MJ, Fischer S, Gao J, Guo H, Ha S, and others. All-atom empirical potential for molecular modeling and dynamics studies of proteins. J Phys Chem B 1998;102:3586–3616.
18. Hubbard RE, Thornton JM. NACCESS. Computer Program. University College London, Department of Biochemistry and Molecular Biology. 1993.
19. Lee B, Richards FM. The interpretation of protein structures: estimation of static accessibility. J Mol Biol 1971;55:379–400.
20. Janin J. Surface and inside volumes in globular proteins. Nature 1979;277:491–492.
21. Gothel SF, Marahiel MA. Peptidyl-prolyl cis-trans isomerases, a superfamily of ubiquitous folding catalysts. Cell Mol Life Sci 1999;55:423–436.
22. Futer O, DeCenzo MT, Aldape RA, Livingston DJ. FK506 binding protein mutational analysis. Defining the surface residue contributions to stability of the calcineurin co-complex. J Biol Chem 1995;270:18935–18940.
23. DeCenzo MT, Park ST, Jarrett BP, Aldape RA, Futer O, Murcko MA, Livingston DJ. FK506-binding protein mutational analysis: defining the active-site residue contributions to catalysis and the stability of ligand complexes. Protein Eng 1996;9:173–180.
24. Clackson T, Yang W, Rozamus LW, Hatada M, Amara JF, Rollins CT, Stevenson LF, Magari SR, Wood SA, Courage NL, and others. Redesigning an FKBP-ligand interface to generate chemical dimerizers with novel specificity. Proc Natl Acad Sci USA 1998;95:10437–10442.
25. Michnick SW, Rosen MK, Wandless TJ, Karplus M, Schreiber SL. Solution structure of FKBP, a rotamase enzyme and receptor for FK506 and rapamycin. Science 1991;252:836–839.
26. Van Duyne GD, Standaert RF, Karplus PA, Schreiber SL, Clardy J. Atomic structures of the human immunophilin FKBP-12 complexes with FK506 and rapamycin. J Mol Biol 1993;229:105–124.
27. Burkhard P, Taylor P, Walkinshaw MD. X-ray structures of small ligand-FKBP complexes provide an estimate for hydrophobic interaction energies. J Mol Biol 2000;295:953–962.
28. Liang J, Hung DT, Schreiber SL, Clardy J. Structure of the human 25 kDa FK506 binding protein complexed with rapamycin. J Am Chem Soc 1996;118:1231–1232.
29. Fulton KF, Jackson SE, Buckle AM. Energetic and structural analysis of the role of tryptophan 59 in FKBP12. Biochemistry 2003;42:2364–2372.
30. Bryson JW, Desjarlais JR, Handel TM, DeGrado WF. From coiled coils to small globular proteins: Design of a native-like three-helix bundle. Protein Sci 1998;7:1404–1414.
31. Hendsch ZS, Jonsson T, Sauer RT, Tidor B. Protein stabilization by removal of unsatisfied polar groups: computational approaches and experimental tests. Biochemistry 1996;35:7621–7625.
32. Waldburger CD, Jonsson T, Sauer RT. Barriers to protein folding: formation of buried polar interactions is a slow step in acquisition of structure. Proc Natl Acad Sci USA 1996;93:2629–2634.
33. Cupp-Vickery JR, Han O, Hutchinson CR, Poulos TL. Substrate-assisted catalysis in cytochrome P450eryF. Nat Struct Biol 1996;3: 632–637.
34. Shaltiel S, Cox S, Taylor SS. Conserved water molecules contribute to the extensive network of interactions at the active site of protein kinase A. Proc Natl Acad Sci USA 1998;95:484–491.
35. Miller MD, Cai J, Krause KL. The active site of Serratia endonuclease contains a conserved magnesium-water cluster. J Mol Biol 1999;288:975–987.
36. Hubbard SJ, Argos P. A functional role for protein cavities in domain: domain motions. J Mol Biol 1996;261:289–300.
37. Petrone PM, Garcia AE. MHC-peptide binding is assisted by bound water molecules. J Mol Biol 2004;338:419–435.
38. Finney JL. The organization and function of water in protein crystals. Philos Trans R Soc Lond B Biol Sci 1977;278:3–32.
39. Edsall JT, McKenzie HA. Water and proteins. II. The location and dynamics of water in protein systems and its relation to their stability and properties. Adv Biophys 1983;16:53–183.
40. Sreenivasan U, Axelsen PH. Buried water in homologous serine proteases. Biochemistry 1992;31:12785–12791.
41. Loris R, Langhorst U, De Vos S, Decanniere K, Bouckaert J, Maes D, Transue TR, Steyaert J. Conserved water molecules in a large family of microbial ribonucleases. Proteins 1999;36:117–134.
42. Eriksson AE, Baase WA, Zhang XJ, Heinz DW, Blaber M, Baldwin EP, Matthews BW. Response of a protein structure to cavity-creating mutations and its relation to the hydrophobic effect. Science 1992;255:178–183.
43. Buckle AM, Henrick K, Fersht AR. Crystal structural analysis of mutations in the hydrophobic cores of barnase. J Mol Biol 1993;234:847–860.
44. Takano K, Funahashi J, Yamagata Y, Fujii S, Yutani K. Contribution of water molecules in the interior of a protein to the conformational stability. J Mol Biol 1997;274:132–142.
45. Xu J, Baase WA, Quillin ML, Baldwin EP, Matthews BW. Structural and thermodynamic analysis of the binding of solvent at internal sites in T4 lysozyme. Protein Sci 2001;10:1067–1078.
46. Covalt JC Jr, Roy M, Jennings PA. Core and surface mutations affect folding kinetics, stability and cooperativity in IL-1 beta: does alteration in buried water play a role? J Mol Biol 2001;307: 657–669.
47. Berndt KD, Beunink J, Schroder W, Wuthrich K. Designed replacement of an internal hydration water molecule in BPTI: structural and functional implications of a glycine-to-serine mutation. Biochemistry 1993;32:4564–4570.
48. Lett CM, Berghuis AM, Frey HE, Lepock JR, Guillemette JG. The role of a conserved water molecule in the redox-dependent thermal stability of iso-1-cytochrome c. J Biol Chem 1996;271: 29088–29093.
49. Quillin ML, Arduini RM, Olson JS, Phillips GN Jr. High-resolution crystal structures of distal histidine mutants of sperm whale myoglobin. J Mol Biol 1993;234:140–155.
50. Blake CC, Pulford WC, Artymiuk PJ. X-ray studies of water in crystals of lysozyme. J Mol Biol 1983;167:693–723.
51. Richards FM. The interpretation of protein structures: total volume, group volume distributions and packing density. J Mol Biol 1974;82:1–14.
52. Ernst JA, Clubb RT, Zhou HX, Gronenborn AM, Clore GM. Demonstration of positionally disordered water within a protein hydrophobic cavity by NMR. Science 1995;267:1813–1817.
53. Otting G, Liepinsh E, Wuthrich K. Protein hydration in aqueous solution. Science 1991;254:974–980.
54. Brunne RM, Berndt KD, Guntert P, Wuthrich K, van Gunsteren WF. Structure and internal dynamics of the bovine pancreatic trypsin inhibitor in aqueous solution from long-time molecular dynamics simulations. Proteins 1995;23:49–62.
55. Garcia AE, Hummer G. Water penetration and escape in proteins. Proteins 2000;38:261–272.
56. Tarek M, Tobias DJ. The dynamics of protein hydration water: a quantitative comparison of molecular dynamics simulations and neutron-scattering experiments. Biophys J 2000;79:3244–3257.
57. Denisov VP, Halle B, Peters J, Horlein HD. Residence times of the buried water molecules in bovine pancreatic trypsin inhibitor and its G36S mutant. Biochemistry 1995;34:9046–90451.
58. Brunne RM, Liepinsh E, Otting G, Wuthrich K, van Gunsteren WF. Hydration of proteins. A comparison of experimental residence times of water molecules solvating the bovine pancreatic trypsin inhibitor with theoretical model calculations. J Mol Biol 1993;231:1040–1048.
59. Higo J, Nakasako M. Hydration structure of human lysozyme investigated by molecular dynamics simulation and cryogenic X-ray crystal structure analyses: on the correlation between crystal water sites, solvent density, and solvent dipole. J Comput Chem 2002;23:1323–1336.
60. Massi F, Straub JE. Structural and dynamical analysis of the hydration of the Alzheimer's beta-amyloid peptide. J Comput Chem 2003;24:143–153.
61. Sanjeev BS, Vishveshwara S. Protein-water interactions in ribonuclease A and angiogenin: a molecular dynamics study. Proteins 2004;55:915–923.
62. Wade RC, Mazor MH, McCammon JA, Quiocho FA. A molecular dynamics study of thermodynamic and structural aspects of the hydration of cavities in proteins. Biopolymers 1991;31:919–931.
63. Likic VA, Juranic N, Macura S, Prendergast FG. A "structural" water molecule in the family of fatty acid binding proteins. Protein Sci 2000;9:497–504.
64. Higo J, Sasai M, Shirai H, Nakamura H, Kugimiya T. Large vortex-like structure of dipole field in computer models of liquid water and dipole-bridge between biomolecules. Proc Natl Acad Sci USA 2001;98:5961–5964.
65. Guex N, Peitsch MC. SWISS-MODEL and the Swiss-PdbViewer: an environment for comparative protein modeling. Electrophoresis 1997;18:2714–2723.